Heliyon 10 (2024) e32014

Contents lists available at ScienceDirect

Heliyon

journal homepage: www.cell.com/heliyon

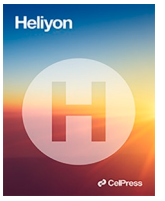

Research article

# METTL14 inhibits the malignant processes of gastric cancer cells by promoting N6-methyladenosine (m6A) methylation of TAF10

Xin Zhao [a,*,1], Jingfen Lu [b,1], Weimin Wu [a], Jiahui Li [c]

[a] *Department of General Surgery, The 928th Hospital of the Joint Logistic Support Force of the People's Liberation Army, 100 Longkun South Road, Longhua District, Haikou, 570100, Hainan, China*
[b] *Department of Hemato-oncology, The 928th Hospital of the Joint Logistic Support Force of the People's Liberation Army, 100 Longkun South Road, Longhua District, Haikou, 570100, Hainan, China*
[c] *Department of Medical Imaging, The 74th Military Medical Hospital of Chinese People's Liberation Army CN, 468 Xingang Middle Road, Haizhu District, Guangzhou, 510318, Guangdong, China*

ARTICLE INFO

*Keywords:*
Gastric cancer
METTL14
m6A methylation
TAF10
Cell proliferation
Migration
Invasion

ABSTRACT

N6-methyladenosine (m6A) methylation mediates cancer development by regulating cell proliferation and metastasis. This study aimed to identify whether methyltransferase 14 (METTL14) affects gastric cancer (GC) cellular functions and its underlying mechanism. METTL14 and TATA-box binding protein associated factor 10 (TAF10) levels were examined using quantitative real-time PCR, immunohistochemical assay, and Western blot. Biological functions were assessed using cell counting kit-8, colony formation, and transwell assays. The interaction between METTL14 and TAF10 was analyzed using RNA immunoprecipitation, methylated RNA immunoprecipitation, and luciferase reporter assay. A xenograft tumor mouse model was established to assess the role of METTL14 *in vivo*. The results suggested that METTL14 was low expressed and TAF10 was highly expressed in GC tissues and cells. METTL14 overexpression inhibited GC cell viability, colony, migration, and invasion. TAF10 was predicted and confirmed to be negatively related to METTL14. METTL14 promoted m6A methylation of TAF10 and inhibited TAF10 stability. Moreover, TAF10 counteracted the cellular behaviors regulated by METTL14. Overexpression of METTL14 inhibited tumor growth and histopathology. In conclusion, METTL14 inhibits GC progression by attenuating GC cell proliferation, migration, and invasion. Mechanistically, METTL14 promoted m6A methylation of TAF10, suppressed the stability of TAF10, and thus downregulated the TAF10 levels, These results provide a new insight into GC therapy.

## 1. Introduction

Gastric cancer (GC) is one of the common causes of cancer deaths globally. With an incidence of more than 1 million people per year, GC is still prevalent in developing countries, particularly in East Asia including China, even though its incidence has declined in the USA [1]. Helicobacter pylori infection, aging, and unhealthy diet are risk factors for GC [2]. The disease is usually diagnosed at an advanced stage after distant metastasis. Multidisciplinary therapies including surgery, chemoradiotherapy, targeted therapy, and immunotherapy are the standard treatment of GC [3]. Despite tremendous development in GC treatment strategies, due to the distant

* Corresponding author.
*E-mail address:* Drzhaox131@163.com (X. Zhao).
[1] These authors contributed equally to this work and should be considered co-first authors.

https://doi.org/10.1016/j.heliyon.2024.e32014
Received 28 January 2024; Received in revised form 26 May 2024; Accepted 27 May 2024
Available online 28 May 2024

metastasis and drug resistance, patients with advanced disease have an extremely poor prognosis, with an overall survival of only about 1 year [4]. Therefore, revealing the molecular mechanism of GC metastasis will contribute to decelerating the progression of GC to the advanced stage and provide a new prospect for a cure.

N6-methyladenosine (m6A) methylation is a RNA post-transcriptional modification that is dynamic and reversible [5]. It participates in multiple RNA processes such as translation, transcription, splicing, degradation, and stability. M6A methylation is mediated by methyltransferases "writers", demethylase "erasers", and methylation recognition proteins "readers". Aberrant m6A modification is commonly seen in tumors and is involved in tumor growth, metastasis, angiogenesis, and immunity [6]. Methyltransferase-like 3 (METTL3), METTL14, and WTAP are the main "writers" in m6A modification. It is required to maintain METTL3-METTL14 complex integrity and recognize specific RNA substrates. In general, METTL14 together with METTL3 functions on m6A [7]. METTL3 is the main catalytic subunit of m6A modification, and METTL14 affects the catalytic activity of METTL3 [8]. Accumulating evidence has revealed that METTL14 is associated with cancer development and tumorigenesis, functioning as an oncogene or a tumor suppressor. For example, depletion of METTL14 promotes cellular proliferation, invasion, and tumorigenicity of colorectal cancer [9]. Upregulation of METTL14 in pancreatic cancer promotes tumor growth and metastasis [10]. Additionally, METTL14 suppresses tumor cell growth and metastasis to impede GC progression [11,12]. Nevertheless, METTL14 regulated molecular mechanism has not yet been fully revealed.

TATA-box binding protein associated factor 10 (TAF10) occurs lysine monomethylation *in vivo* and regulates development. TAF10 is a subunit of transcription factor IID (TFIID), which is a transcription factor to form a pre-initiation complex on the promoter and regulates eukaryotic transcription [13]. Methylation of TAF10 enhances affinity for RNA polymerase II, facilitating TAF10 transcription [14]. Cells that do not express TAF10 cannot survive because their cell cycle is blocked and leads to apoptosis [15]. However, the role of TAF10 in GC remains not understood due to it is less studied in tumors.

Here, we clarified whether METTL14 influences TAF10 to regulate GC progression. We found that METTL14 was downregulated and TAF10 was upregulated in GC. Overexpression of METTL14 promoted TAF10 m6A methylation and further reduced its stability to inhibit GC cell proliferation, invasion, and migration. The data indicated an important role of the METTL14/TAF10 axis in GC.

## 2. Materials and methods

### 2.1. Tissue specimens

Paired GC tissues and adjacent normal tissues (para-GC) were obtained from patients diagnosed with GC (n = 63) during surgery in the 928th Hospital of the Joint Logistic Support Force of the People's Liberation Army from January to July 2018. Patient inclusion criteria were: 1) patients who were first diagnosed with GC by histopathology; 2) patients without other malignant tumors; 3) patients had not undergone any form of anti-cancer therapy; 4) patients had no organ dysfunction; 5) patients had no autoimmune disease. They provided written informed consent pre-operation. The obtained tissues were all stored at −80 °C. The study was reviewed and approved by the Ethics Committee of the 928th Hospital of the Joint Logistic Support Force of the People's Liberation Army, with the approval number: 2023-KYL-01. Follow-up of these patients lasted 60 months. Drop-out cases at follow-up and patients who did not die before the end of follow-up were considered to be censored observations. The clinical characteristics of patients with high or low

**Table 1**
Correlation between METTL14 expression and clinicopathological characteristics of GC patients.

| Variables | Low (n = 31) | High (n = 32) | $X^2$ | P |
|---|---|---|---|---|
| Age (years) | | | 0.021 | 0.884 |
| <65 | 18 | 18 | | |
| ≥65 | 13 | 14 | | |
| Sex | | | 1.073 | 0.300 |
| Female | 7 | 11 | | |
| Male | 24 | 21 | | |
| BMI | | | 0.075 | 0.784 |
| ≤25 | 26 | 26 | | |
| >25 | 5 | 6 | | |
| Tumor size (mm) | | | 4.585 | 0.032* |
| < 50 | 13 | 22 | | |
| ≥50 | 18 | 10 | | |
| Tumor location | | | 1.157 | 0.763 |
| Upper | 10 | 7 | | |
| Middle | 5 | 5 | | |
| Low | 13 | 15 | | |
| Overlap | 3 | 5 | | |
| Histological grade | | | 4.661 | 0.031* |
| Well/Moderately | 10 | 19 | | |
| Poor | 21 | 13 | | |
| TNM stage | | | 4.763 | 0.029* |
| I&II | 9 | 18 | | |
| III&IV | 22 | 14 | | |

METTL14 expression are shown in Table 1.

### 2.2. Cell culture and transfection

Human GC cells (AGS, HGC27, N87, and MKN74) and human gastric mucosa cells (GES1) were acquired from ATCC (Manassas). They were maintained in DMEM/F12 (Hyclone, South Logan) supplemented with 10 % FBS and 1 % penicillin/streptomycin (Gibco, Grand Island) at 37 °C with 5 % $CO_2$.

AGS and HGC27 cells were incubated at 37 °C for 24 h after seeding in 6-well plates. METTL14 overexpression vector (oe-METTL14), oe-TAF10, oe-negative control (nc), METTL14 short hairpin RNA (sh-METTL14), and sh-nc were purchased from GenePharma (Shanghai) and were transfected into GC cells in the serum-free medium using Lipofectamine 2000 (Invitrogen, Carlsbad). After 6 h, complete medium was used to replace the current medium. After 48 h, the transfected cells were harvested.

### 2.3. Quantitative real-time PCR (qRT-PCR)

A Total RNA Extraction kit (Tiangen, Beijing) was used to isolate total RNA. Then, reverse transcription to synthesize cDNA was conducted using a FastKing RT Kit (With gDNase) (Tiangen). Afterward, a FastFire qPCR PreMix (SYBR Green) (Tiangen) was utilized for quantification. The fold change of mRNAs was calculated using the $2^{-\Delta\Delta CT}$ method. GAPDH was a normalization for expression calculation.

### 2.4. Cell counting kit-8 (CCK-8) analysis

AGS and HGC27 cells were grown in 96-well plates until 80 % confluence. Cells after transfection were incubated for specified times (0, 24, 48, and 72 h) at 37 °C. CCK-8 reagent (10 μl; Dojindo) was further incubated with the cells for 4 h. Finally, the absorbance at 450 nm was detected under a microplate reader (Bio-Rad, Hercules).

### 2.5. Colony formation analysis

AGS and HGC27 cells were seeded in 6-well plates and maintained in a cell incubator for 14 days. Subsequently, the 0.1 % crystal violet-stained cells were visualized under a light microscope (Olympus, Tokyo).

### 2.6. Transwell assay

Transfected cells were resuspended in the serum-free medium and then added to Matrigel-coated or uncoated upper chambers (8-μm pore size) for invasion or migration analysis. FBS-supplemented DMEM/F12 was used to fill the bottom layer of the chambers. After incubation for 24 h, unmigrated or uninvaded cells were removed by sterile swabs. The other cells were fixed with 4 % paraformaldehyde (Sigma-Aldrich) and stained with crystal violet (Sigma-Aldrich). The stained cells were observed under a microscope (Olympus).

### 2.7. Western blot

Tissue specimens and cells were lysed using RIPA buffer (Beyotime, Shanghai), and a BCA kit (Beyotime) was used to detect protein concentration. The protein (30 μg) was loaded on 10 % SDS-PAGE and transferred to PVDF membranes (Millipore, Billerica). Following blocking, primary antibodies (anti-METTL14, anti-TAF10, anti-GAPDH) were incubated with the membranes at 4 °C overnight, and the secondary antibody was further incubated with the membranes at room temperature for 1 h. A Clarity Western electro-chemiluminescence (ECL) Substrate (Bio-Rad) was used to develop each protein band. GAPDH was used for internal normalization.

### 2.8. Bioinformatic analysis

METTL14-associated mRNAs were predicted using the LinkedOmics online database (http://www.linkedomics.org/login.php). The GEPIA (http://gepia.cancer-pku.cn/), linkedomics, and starBase (https://starbase.sysu.edu.cn/starbase2/index.php) online tools were used to evaluate the correlation between METTL14 and TAF10. The m6A methylation sites in TAF10 were acquired from the SRAMP database (http://www.cuilab.cn/sramp).

### 2.9. RNA immunoprecipitation (RIP) analysis

RIP was conducted to assess the binding relationship using a RIP kit (Geneseed, Guangzhou). Transfected cells were treated with a lysis buffer on ice for 10 min, and the supernatant was collected following centrifugation. On the other hand, Protein A + G beads were connected to anti-METTL14 and anti-IgG at 4 °C for 2 h, followed by incubation with the supernatant at 4 °C overnight. After the magnetic beads were eluted, total RNA was isolated and the levels of TAF10 were examined using qRT-PCR.

### 2.10. Methylated RNA immunoprecipitation (MeRIP) analysis

MeRIP was conducted to detect m6A enrichment of TAF10 using a MeRIP kit (Ribobio, Guangzhou). The transfected cells were digested with DNase I. Total RNA was extracted, disrupted, and collected. On the other hand, the magnetic beads A/G were incubated with anti-IgG and anti-m6A for 1 h. Then, the fragmented RNA was incubated with RNase inhibitor, IP buffer, and beads-antibody complex at 4 °C overnight. After washing, TAF10 expression was measured using qRT-PCR.

### 2.11. Dual-luciferase reporter assay

Wild-type and mutant sequences of TAF10 (wt-TAF10, UUAAUGGACUGUCUU; and mut-TAF10, UUAUUGGUCUGUCUU) were inserted into the pGL3 plasmid (Promega, Madison). GC cells were co-cultured with wt-TAF10 or mut-TAF10 together with oe-nc or oe-METTL14 using Lipofectamine 3000. After 48 h, firefly and Renilla luciferase activities were measured using the Dual-Luciferase Reporter Assay System (Promega).

### 2.12. Measurement of TAF10 stability

The transfected AGS and HGC27 cells were exposed to 2 μg/mL actinomycin D (AAT Bioquest, Sunnyvale) for different times (0, 1, 2, 4, and 8 h). TAF10 expression was measured using qRT-PCR.

### 2.13. In vivo study

Male BALB/c nude mice (4–6 weeks old, 18–22 g) were purchased from Shanghai Experimental Animal Center (Shanghai) and randomly divided into 2 groups: lentivirus (Lv)-NC and Lv-METTL14 group, with six mice per group. AGS cells were stably transfected with Lv-NC or Lv-METTL14 (GenePharma) using Lipofectamine 3000. To analyze tumor growth *in vivo*, approximately $1 \times 10^7$ transfected cells were subcutaneously injected into the flank of nude mice. When the tumor volume reached 100 $mm^3$, this day was defined as day 1. Then, tumor volume was detected every week using the formula (Width2 × Length)/2. After 28 days, all mice were sacrificed and the tumors were photographed. Tumor weight was measured. To analyze tumor metastasis *in vivo*, $5 \times 10^6$ transfected cells that were suspended in 100 μl PBS were injected into the tail veins of mice. After 60 days, all mice were sacrificed. The lungs were collected from each mouse. The procedures associated with mice were approved by the Ethics Committee of the 928th Hospital of the Joint Logistic Support Force of the People's Liberation Army, with the approval number: 2023-KYL-01. The animal experiments were performed in accordance with the ARRIVE guidelines.

### 2.14. H&E staining assay

Tumor tissues were fixed in formalin, embedded in paraffin, and then prepared into 5 μm paraffin sections. The sections were deparaffinated and rehydrated. Then, the sections were incubated with hematoxylin and eosin (Sigma-Aldrich), and viewed under a light microplate (Olympus).

### 2.15. Immunohistochemical (IHC) analysis

The levels of METTL14 and TAF10 in human clinical tissues, as well as the levels of ki67 and TAF10 in tumor tissues, were measured using IHC analysis. Briefly, GC and para-GC tissues from patients, and tumor tissues from mice were sliced into paraffin sections. The sections were deparaffinized to water, and incubated with 3 % $H_2O_2$ for 5 min, followed by blocking with 5 % normal serum. Anti-METTL14, anti-TAF10, and anti-ki67 were incubated with the sections overnight at 4 °C, and then incubated with secondary antibody for 0.5 h at 37 °C. Following staining with the DAB solution (Sigma-Aldrich), the sections were viewed using a light microplate (Olympus).

### 2.16. Statistical analysis

The data were analyzed using the GraphPad Prism 7 software (GraphPad Software, San Diego) and shown as mean ± standard deviation. The diagnostic value of METTL14 in GC was assessed using ROC curve analysis. The survival analysis was determined using Kaplan-Meier curves. Correlation analysis between genes was determined by the Pearson correlation coefficient. The significance of data variation was evaluated using Student's t-test or one-way ANOVA. $P < 0.05$ indicates a significant difference in data.

## 3. Results

### 3.1. Downregulation of METTL14 in GC

M6A methylation is involved in the development of cancers. METTL14 is an m6A "writer" that promotes mRNA m6A methylation. Previous studies have revealed that METTL14 contributes to decelerating GC progression. To confirm the role of METTL14 in GC, we first measured the expression of METTL14 in GC. The data of qPCR showed lower expression of METTL14 in GC tissues than that in

para-GC tissues (P < 0.0001; Fig. 1A). The diagnostic value of METTL14 was determined using the ROC curve, and the results showed that the AUC value was 0.8653, greater than 0.8 (Fig. 1B), suggesting that METTL14 is a promising diagnostic biomarker of GC. We conducted a survey of the correlation between GC patients with high or low METTL14 expression and clinicopathological characteristics. As shown in Table 1, high METTL14 expression was associated with small tumor size, well/moderate histological grade, and early TNM stage; however, METTL14 expression was not related to age, sex, BMI, and tumor location. After five years of follow-up, 50 patients died. The other patients were censored at the end of the study or dropped out. GC patients with low METTL14 expression had a worse prognosis than those with low METTL14 expression (p = 0.0175; Fig. 1C). The data of the IHC assay showed that METTL14 levels were decreased in GC tissues (Fig. 1D). Additionally, METTL14 expression was reduced in GC cells such as AGS, HGC27, N87, and MKN74 cells, compared with GES1 cells (Fig. 1E). Similar to the mRNA level, METTL14 at the protein levels was also downregulated in GC cells (Fig. 1F). Collectively, METTL14 is downregulated in GC, suggesting that METTL14 may be a tumor suppressor in GC.

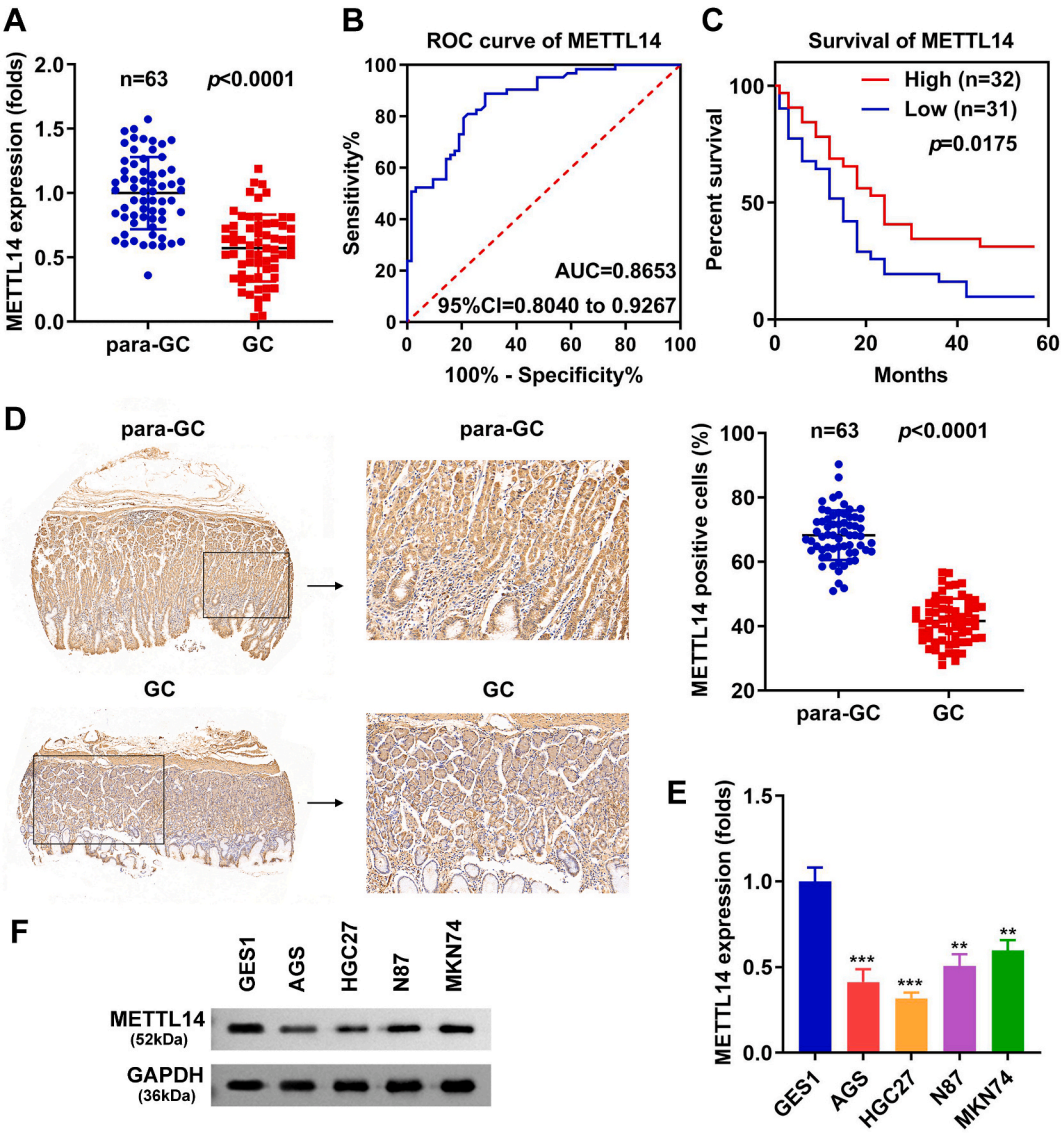


**Fig. 1.** Low expression ofMETTL14 in GC. (A) qRT-PCR was performed to test METTL14 expression in tumor tissues and para-GC tissues (63 pairs). (B) The ROC curve of METTL14 for diagnosis of GC and AUC value was calculated. (C) Kaplan-Meier curves for the survival of GC patients with high or low expressed METTL14. (D) IHC assay was used to analyze METTL14 levels in clinical tissues. METTL14 expression in GES1, AGS, HGC27, N87, and MKN74 cells was detected using (E) qRT-PCR and (F) Western blot. The original protein bands are shown in Supplementary Fig. 2. **P < 0.01. ***P < 0.001.

### 3.2. Overexpression of METTL14 inhibits malignant GC cell behaviors

To investigate the functional role of METTL14, we transfected oe-nc and oe-METTL14 into AGS and HGC27 cells. After transfection with oe-METTL14, METTL14 levels were significantly increased (Fig. 2A). The viability of GC cells in the METTL14 group was markedly inhibited (Fig. 2B). Overexpression of METTL14 significantly reduced GC cell colonies, compared with oe-nc (Fig. 2C). The migratory capability was dramatically inhibited by METTL14 overexpression (Fig. 2D). Cell invasion ability was also notably suppressed in the oe-METTL14 group (Fig. 2E). In addition, to assess the effect of METTL14 knockdown on cellular behaviors, sh-METTL14 and sh-nc were transfected into N87 and MKN74 cells. As shown in Fig. S1A, METTL14 expression was downregulated after sh-METTL14 transfection, compared with sh-nc. Next, the results showed that knockdown of METTL14 promoted N87 and MKN74 cell viability (Fig. S1B), colonies (Fig. S1C), migration (Fig. S1D), and invasion (Fig. S1E). The results demonstrate that METTL14 suppresses GC cell proliferation, migration, and invasion.

### 3.3. The interaction between METTL14 and TAF10

Then, we identified METTL14-related mRNAs and found that numerous genes were positively or negatively correlated to METTL14 (Fig. 3A–C). To explore the underlying mechanism of METTL14, we chose TAF10, the most significantly negatively correlated gene to METTL14, for further study (Fig. 3C). Correlation analysis using bioinformatic analysis showed that METTL14 was negatively related to TAF10 in GC (Fig. 3D–F). The results indicate that TAF10 expression is predicted to be negatively related to METTL14 expression.

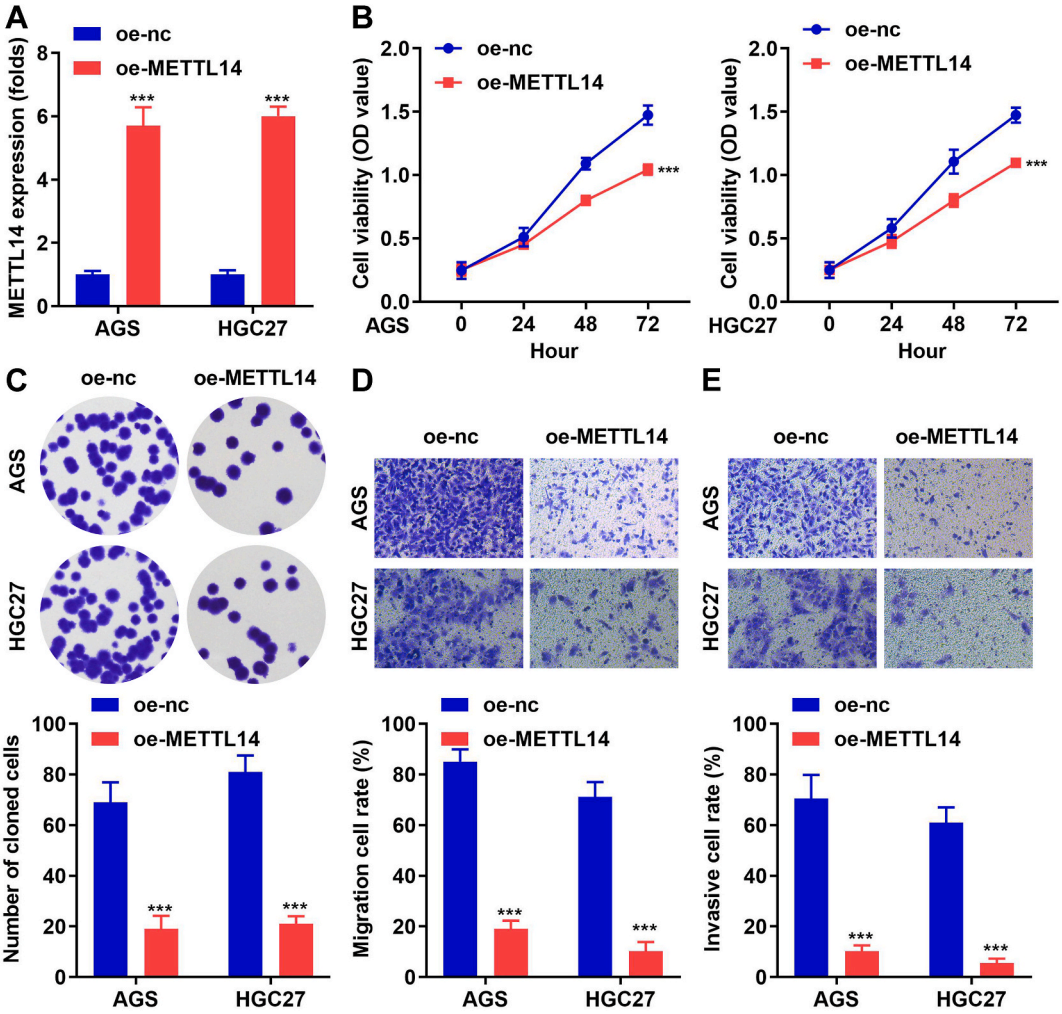


**Fig. 2.** METTL14 inhibits GC cell proliferation and metastasis. (A) METTL14 expression was measured using qRT-PCR following transfection. (B) Cell proliferation was assessed by detecting (B) cell viability using CCK-8 and (C) cell colonies using colony formation, respectively. Cell migratory (D) and invasive (E) capabilities were detected by Transwell assay. ***P < 0.001.

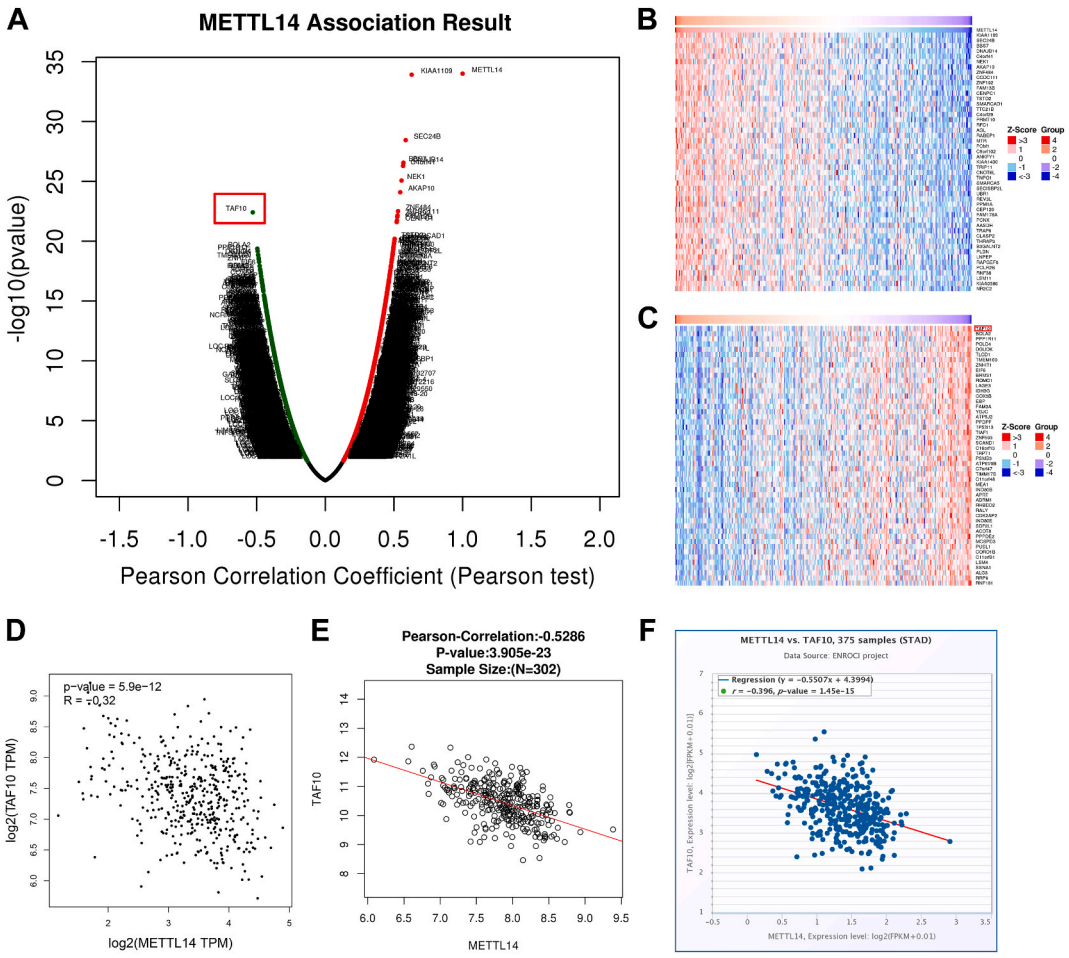


**Fig. 3.** The prediction of interaction between METTL14 and TAF10. (A) METTL14 positive and negative related genes were predicted using the LinkedOmics database. (B) METTL14-positive related genes were shown using the heatmap. (C) METTL14-negative related genes were shown using the heatmap. The correlation between METTL14 and TAF10 was predicted using the (D) GEPIA database, (E) Linkedomics database, and (F) starBase database.

### *3.4. Highly expressed TAF10 in GC*

The levels of TAF10 were further examined to confirm the prediction. TAF10 expression was increased in GC tissues (Fig. 4A and C) and was negatively related to METTL14 (Fig. 4B). In addition, TAF10 expression was elevated in AGS, HGC27, N87, and MKN74 cells, especially in AGS and HGC27 cells (Fig. 4D). METTL14 overexpression reduced TAF10 expression in both AGS and HGC27 cells (Fig. 4E and F). To sum up, TAF10 expression is elevated in GC.

### *3.5. METTL14 promotes m6A methylation of TAF10*

METTL14 is a m6A "writer". Therefore, we measured the m6A methylation in TAF10 mediated by METTL14. The interaction between TAF10 and METTL14 was assessed using RIP, and the results showed that TAF10 mRNA combined with METTL14 protein (Fig. 5A). Moreover, overexpression of METTL14 notably promoted m6A methylation modification of TAF10 (Fig. 5B). Multiple methylation sites were predicted in TAF10 (Fig. 5C). The data showed that METTL14 markedly decreased the luciferase activity in the wt-TAF10 group, whereas oe-nc and oe-METTL14 did not influence the luciferase activity co-transfected with mut-TAF10 (Fig. 5D). Generally, m6A methylation affects mRNA degradation and translation. Thus, we measured TAF10 mRNA stability after actinomycin D treatment. METTL14 overexpression inhibited the stability of TAF10 in GC cells (Fig. 5E). Taken together, METTL14 could bind to the methylation sites of TAF10 to promote m6A methylation, promoting TAF10 degradation.

### *3.6. METTL14 inhibits GC malignant progression by downregulating TAF10*

Rescue studies were performed to explore the effects of METTL14 and TAF10 on GC cellular behaviors. oe-nc and oe-TAF10 were

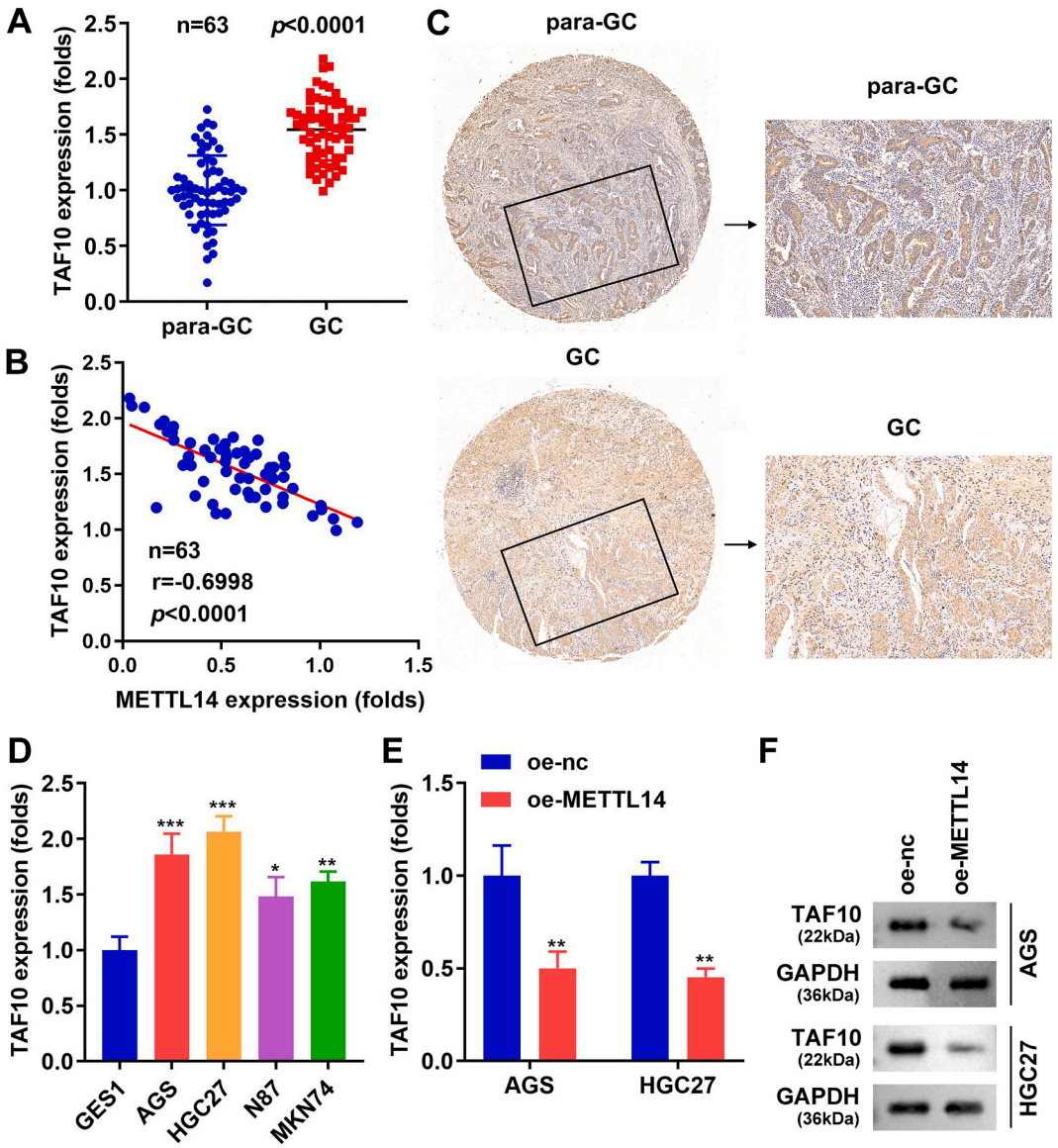


**Fig. 4.** High expression of TAF10 in GC. (A) TAF10 levels in clinical tissues (63 pairs) were tested by qRT-PCR. (B) The correlation between METTL14 and TAF10 in tumor tissues (n = 63) was assessed using the Pearson correlation coefficient. (C) TAF10 expression in tissues was measured using IHC analysis. (D) qRT-PCR was conducted to measure TAF10 expression in GES1, AGS, HGC27, N87, and MKN74 cells. (E) TAF10 expression was detected in oe-nc and oe-METTL14 transfected GC cells using qRT-PCR. (F) TAF10 expression was examined by Western blot after over-expressing METTL14. The original protein bands are shown in Supplementary Fig. 3. *P < 0.05. **P < 0.01. ***P < 0.001.

transfected into AGS and HGC27 cells. We found that TAF10 was significantly elevated following oe-TAF10 transfection (Fig. 6A). Cell viability was notably inhibited by METTL14, which was notably counteracted by TAF10 (Fig. 6B). Overexpression of METTL14 markedly reduced cell colonies, whereas TAF10 markedly abrogated the reduction (Fig. 6C). Additionally, METTL14 notably inhibited GC cell migration, while TAF10 significantly reversed the inhibition of the migration (Fig. 6D). The suppression of invasion induced by METTL14 was significantly reversed by TAF10 (Fig. 6E). The results indicate that METTL14 suppresses the biological behaviors mentioned above by regulating TAF10 expression.

### 3.7. *METTL14 impedes tumor growth and lung metastasis in vivo*

Finally, the role of METTL14 *in vivo* was evaluated in xenograft tumor mice and lung metastasis mice. The results showed that overexpression of METTL14 reduced tumor size, tumor weight, and tumor volume (Fig. 7A–C). Then, H&E staining revealed the tumor histopathology. METTL14 overexpression improved tumor pathology (Fig. 7D). In addition, Ki67 and TAF10 levels were decreased by

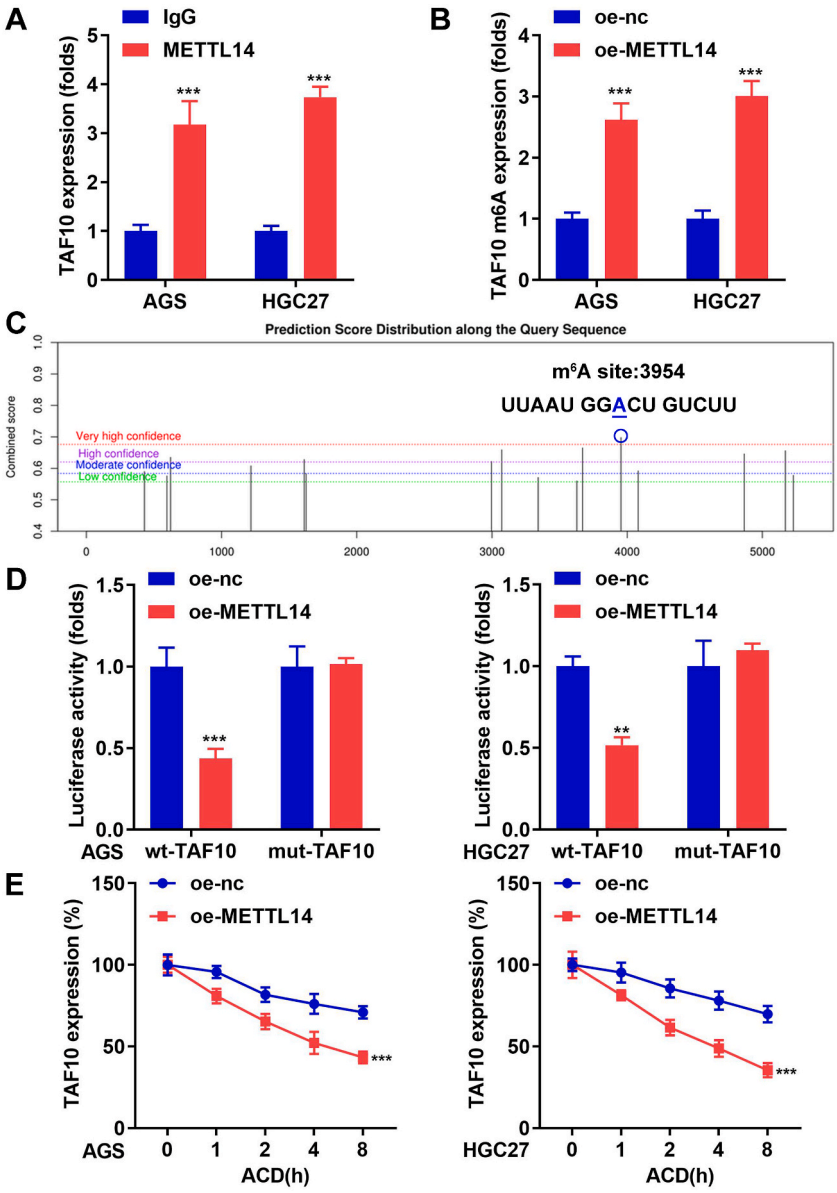


**Fig. 5.** METTL14 promotes m6A methylation of TAF10. (A) RIP was used to assess TAF10 mRNA and METTL14 protein interaction. (B) m6A methylation of TAF10 was analyzed by Me-RIP assay. (C) The methylation sites in TAF10 were obtained from the SRAMP database, and the site studied in this study is shown (D) TAF10 and METTL14 relationship was determined by luciferase reporter assay. (E) TAF10 mRNA stability was tested using qRT-PCR after actinomycin D treatment. **P < 0.01. ***P < 0.001.

METTL14 overexpression, which was measured using IHC assay (Fig. 7D). Moreover, we analyzed the effect of METTL14 on lung metastasis. The results showed that overexpression of METTL14 reduced the metastatic nodules in the lung (Fig. 7E), suggesting that METTL14 inhibits lung metastasis of tumors.

## 4. Discussion

M6A modification is the most common RNA modification in eukaryotes that is mediated by “writer”, “eraser”, and “reader”. METTL3 and METTL14 are the main “writers” catalyzing the m6A methylation. METTL14, a METTL3 homolog, can form a stable heterodimer between them [7,16]. METTL14 is usually dysregulated in malignancy. It is downregulated in colorectum [17], skin [18], and liver cancers [19], but has increased expression in breast [20] and pancreatic cancers [21]. In GC, METTL14 has been proven to have inhibitory effects on cellular proliferation, growth, migration, invasion, and glycolysis [11,12,22,23]. Herein, we clarified that upregulation of METTL14 suppressed GC cell proliferation, migration, and invasion *in vitro*, and inhibited tumor growth *in vivo*. The

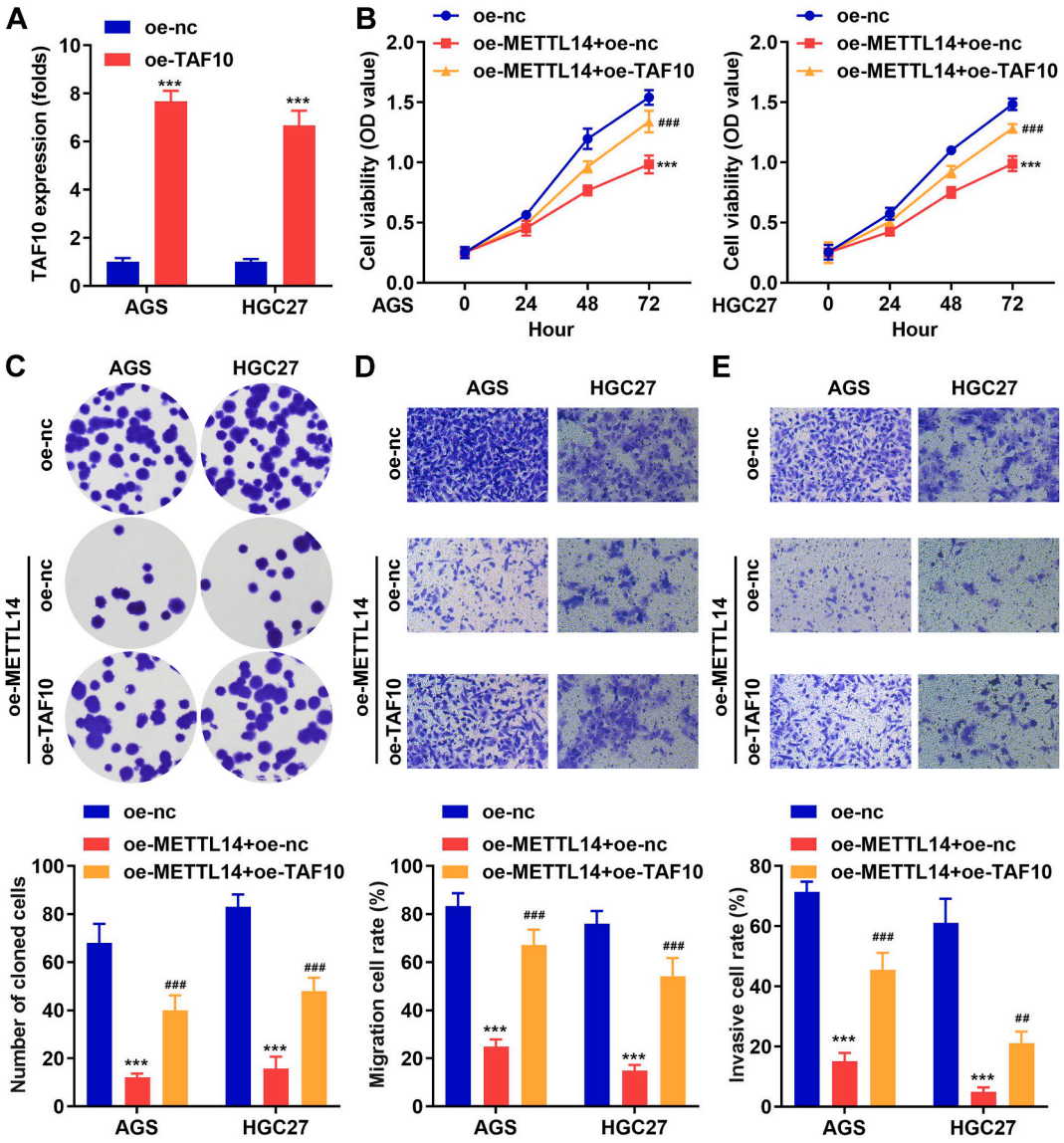


**Fig. 6.** METTL14 inhibits GC malignant progression by downregulating TAF10. (A) qRT-PCR was performed to detect the transfection efficiency after transfection with oe-nc and oe-TAF10 for 48 h. (B) Cell proliferation was assessed by detecting (B) cell viability using CCK-8 and (C) cell colonies using colony formation. Cell migration (D) and invasiveness (E) were detected by Transwell assay. ***P < 0.001. ###P < 0.001.

findings suggest that METTL14 serves as a GC suppressor gene, consistent with previous studies.

METTL14 has been shown to regulate the methylation of non-coding RNAs in GC, such as circORC5 and LINC01320, in previous studies, but the mechanism is still not well understood. Thus, we subsequently studied the underlying mechanisms of METTL14. The data from the bioinformatic analysis revealed that TAF10 was the most significant gene negatively correlated with METTL14. Thus, we investigated the role of TAF10 in GC.

TAF10 is a nuclear transcription factor that modulates cell cycle and endodermal differentiation [15,24]. In addition, TAF10 regulates TFIID stability, cell cycle, and transcription at embryogenesis in mice [25]. However, the role of TAF10 in human diseases is unknown. Herein, we found that TAF10 expression was elevated in GC tissues and cells. We also confirmed that METTL14 was negatively related to TAF10 expression. Thus, we hypothesized that METTL14 regulated GC progression through modulating TAF10 expression. We then examined the methylation of TAF10 and verified this hypothesis with rescue experiments. The results demonstrated that METTL14 promoted m6A methylation of TAF10. Moreover, TAF10 overexpression abrogated the inhibition of cell proliferation and metastasis induced by METTL14. METTL14 has been demonstrated to be involved in RNA stabilization, degradation, pre-RNA splicing, and translation, and thus mediates the advancement of cancers [26,27]. The results indicated that METTL14 facilitated the m6A methylation of TAF10, and further decreased TAF10 stability. Taken together, METTL14 inhibited the progression of GC by promoting the m6A methylation and suppressing the stability of TAF10. However, how TAF10 exerts its oncogenic role in GC

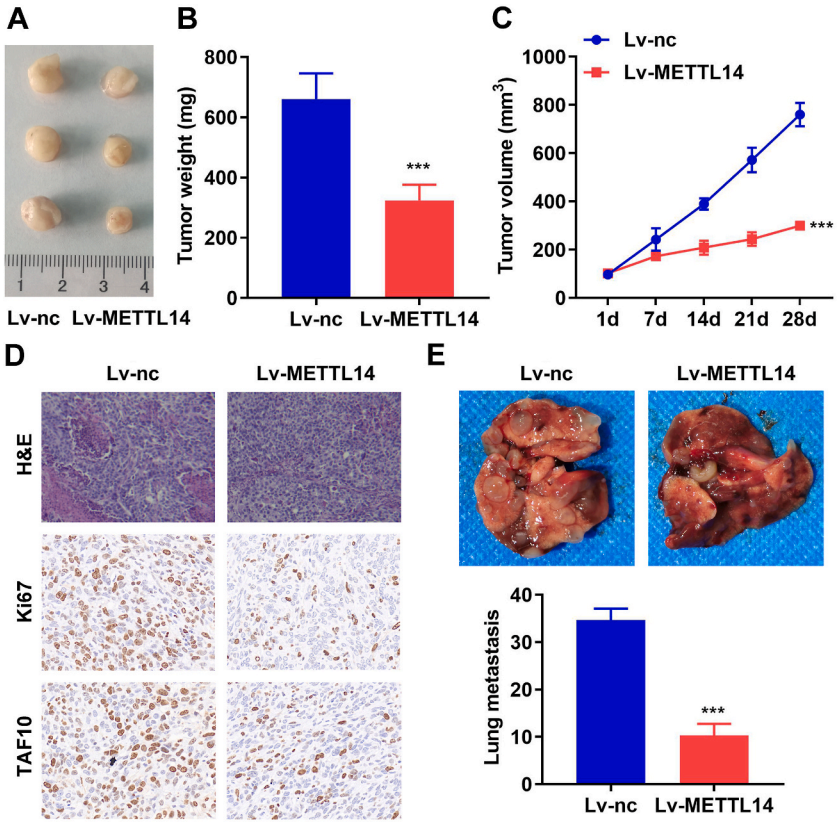


**Fig. 7.** METTL14 impedes tumor growth *in vivo*. (A) Images of representative tumors from mice. (B) Tumor weight of isolated tumors. (C) Tumor volume was detected every 7 days in tumor-bearing mice. (D) H&E staining was used to determine tumor histopathology. Ki67 and TAF10 levels in tumors were measured using IHC analysis. (E) Images of representative lungs from metastasis mouse model, and metastasis nodules were counted. ***P $<$ 0.001.

remains unclear. We will further study the function and mechanism of TAF10 in GC progression.

## 5. Conclusion

In conclusion, METTL14 expression was increased and TAF10 expression was decreased in GC. They have a significant negative correlation. METTL14 inhibited the advancement of GC by inhibiting cell proliferation, migration, and invasion. Mechanically, METTL14 promoted the m6A methylation of TAF10 and inhibited TAF10 stability, thereby reducing the levels of TAF10. We demonstrated that METTL14 may be a diagnostic and prognostic biomarker, and the METTL14/TAF10 axis may be effective in GC therapy. Further, *in vivo* studies are required for its clinical applications.

## Ethics approval and consent to participate

This study was reviewed and approved by the Ethics Committee of the 928th Hospital of the Joint Logistic Support Force of the People's Liberation Army, with the approval number: 2023-KYL-01. All patients provided informed consent to participate in the study. The animal experiments were performed in accordance with the ARRIVE guidelines.

## Consent for publication

All authors approved the final manuscript and the submission to this journal.

## Funding

Not applicable.

## Data availability statement

The datasets used and/or analyzed during the current study are available from the corresponding author upon reasonable request.

## CRediT authorship contribution statement

**Xin Zhao:** Writing – review & editing, Writing – original draft, Conceptualization. **Jingfen Lu:** Formal analysis, Data curation. **Weimin Wu:** Formal analysis, Conceptualization. **Jiahui Li:** Formal analysis, Data curation.

## Declaration of competing interest

The authors declare that they have no known competing financial interests or personal relationships that could have appeared to influence the work reported in this paper.

## Acknowledgements

Not applicable.

## Appendix A. Supplementary data

Supplementary data to this article can be found online at https://doi.org/10.1016/j.heliyon.2024.e32014.

## References

[1] T.H. Patel, M. Cecchini, Targeted therapies in advanced gastric cancer, Curr Treat Options Oncol 21 (9) (2020) 70, https://doi.org/10.1007/s11864-020-00774-4.
[2] E.C. Smyth, M. Nilsson, H.I. Grabsch, N.C. van Grieken, F. Lordick, Gastric cancer, Lancet 396 (10251) (2020) 635–648, https://doi.org/10.1016/S0140-6736(20)31288-5.
[3] S.S. Joshi, B.D. Badgwell, Current treatment and recent progress in gastric cancer, CA Cancer J Clin 71 (3) (2021) 264–279, https://doi.org/10.3322/caac.21657.
[4] A. Digklia, A.D. Wagner, Advanced gastric cancer: current treatment landscape and future perspectives, World J Gastroenterol 22 (8) (2016) 2403–2414, https://doi.org/10.3748/wjg.v22.i8.2403.
[5] T. Wang, S. Kong, M. Tao, S. Ju, The potential role of RNA N6-methyladenosine in Cancer progression, Mol Cancer 19 (1) (2020) 88, https://doi.org/10.1186/s12943-020-01204-7.
[6] N. Zhang, Y. Zuo, Y. Peng, L. Zuo, Function of N6-methyladenosine modification in tumors, J Oncol 2021 (2021) 6461552, https://doi.org/10.1155/2021/6461552.
[7] J. Liu, Y. Yue, D. Han, X. Wang, Y. Fu, L. Zhang, G. Jia, M. Yu, Z. Lu, X. Deng, Q. Dai, W. Chen, C. He, A METTL3-METTL14 complex mediates mammalian nuclear RNA N6-adenosine methylation, Nat Chem Biol 10 (2) (2014) 93–95, https://doi.org/10.1038/nchembio.1432.
[8] H. Zhou, K. Yin, Y. Zhang, J. Tian, S. Wang, The RNA m6A writer METTL14 in cancers: roles, structures, and applications, Biochim Biophys Acta Rev Cancer 1876 (2) (2021) 188609, https://doi.org/10.1016/j.bbcan.2021.188609.
[9] X. Yang, S. Zhang, C. He, P. Xue, L. Zhang, Z. He, L. Zang, B. Feng, J. Sun, M. Zheng, METTL14 suppresses proliferation and metastasis of colorectal cancer by down-regulating oncogenic long non-coding RNA XIST, Mol Cancer 19 (1) (2020) 46, https://doi.org/10.1186/s12943-020-1146-4.
[10] M. Wang, J. Liu, Y. Zhao, R. He, X. Xu, X. Guo, X. Li, S. Xu, J. Miao, J. Guo, H. Zhang, J. Gong, F. Zhu, R. Tian, C. Shi, F. Peng, Y. Feng, S. Yu, Y. Xie, J. Jiang, M. Li, W. Wei, C. He, R. Qin, Upregulation of METTL14 mediates the elevation of PERP mRNA $N^6$ adenosine methylation promoting the growth and metastasis of pancreatic cancer, Mol Cancer 19 (1) (2020) 130, https://doi.org/10.1186/s12943-020-01249-8.
[11] H.N. Fan, Z.Y. Chen, X.Y. Chen, M. Chen, Y.C. Yi, J.S. Zhu, J. Zhang, METTL14-mediated $m^6A$ modification of circORC5 suppresses gastric cancer progression by regulating miR-30c-2-3p/AKT1S1 axis, Mol Cancer 21 (1) (2022) 51, https://doi.org/10.1186/s12943-022-01521-z.
[12] X. Liu, M. Xiao, L. Zhang, L. Li, G. Zhu, E. Shen, M. Lv, X. Lu, Z. Sun, The m6A methyltransferase METTL14 inhibits the proliferation, migration, and invasion of gastric cancer by regulating the PI3K/AKT/mTOR signaling pathway, J Clin Lab Anal 35 (3) (2021) e23655, https://doi.org/10.1002/jcla.23655.
[13] P. Bardot, S.D. Vincent, M. Fournier, A. Hubaud, M. Joint, L. Tora, O. Pourquié, The TAF10-containing TFIID and SAGA transcriptional complexes are dispensable for early somitogenesis in the mouse embryo, Development 144 (20) (2017) 3808–3818, https://doi.org/10.1242/dev.146902.
[14] A. Kouskouti, E. Scheer, A. Staub, L. Tora, I. Talianidis, Gene-specific modulation of TAF10 function by SET9-mediated methylation, Mol Cell 14 (2) (2004) 175–182, https://doi.org/10.1016/s1097-2765(04)00182-0.
[15] D. Metzger, E. Scheer, A. Soldatov, L. Tora, Mammalian TAF(II)30 is required for cell cycle progression and specific cellular differentiation programmes, EMBO J 18 (17) (1999) 4823–4834, https://doi.org/10.1093/emboj/18.17.4823.
[16] J.M. Bujnicki, M. Feder, M. Radlinska, R.M. Blumenthal, Structure prediction and phylogenetic analysis of a functionally diverse family of proteins homologous to the MT-A70 subunit of the human mRNA:m(6)A methyltransferase, J Mol Evol. 55 (4) (2002) 431–444, https://doi.org/10.1007/s00239-002-2339-8.
[17] X. Yang, S. Zhang, C. He, P. Xue, L. Zhang, Z. He, L. Zang, B. Feng, J. Sun, M. Zheng, METTL14 suppresses proliferation and metastasis of colorectal cancer by down-regulating oncogenic long non-coding RNA XIST, Mol Cancer 19 (1) (2020) 46, https://doi.org/10.1186/s12943-020-1146-4.
[18] Z. Yang, S. Yang, Y.H. Cui, J. Wei, P. Shah, G. Park, X. Cui, C. He, Y.Y. He, METTL14 facilitates global genome repair and suppresses skin tumorigenesis, Proc Natl Acad Sci U S A. 118 (35) (2021) e2025948118, https://doi.org/10.1073/pnas.2025948118.
[19] L. Du, Y. Li, M. Kang, M. Feng, Y. Ren, H. Dai, Y. Wang, Y. Wang, B. Tang, USP48 is upregulated by Mettl14 to attenuate hepatocellular carcinoma via regulating SIRT6 stabilization, Cancer Res 81 (14) (2021) 3822–3834, https://doi.org/10.1158/0008-5472.CAN-20-4163.
[20] D. Yi, R. Wang, X. Shi, L. Xu, Y. Yilihamu, J. Sang, METTL14 promotes the migration and invasion of breast cancer cells by modulating N6-methyladenosine and hsa-miR-146a-5p expression, Oncol Rep 43 (5) (2020) 1375–1386, https://doi.org/10.3892/or.2020.7515.
[21] M. Wang, J. Liu, Y. Zhao, R. He, X. Xu, X. Guo, X. Li, S. Xu, J. Miao, J. Guo, H. Zhang, J. Gong, F. Zhu, R. Tian, C. Shi, F. Peng, Y. Feng, S. Yu, Y. Xie, J. Jiang, M. Li, W. Wei, C. He, R. Qin, Upregulation of METTL14 mediates the elevation of PERP mRNA $N^6$ adenosine methylation promoting the growth and metastasis of pancreatic cancer, Mol Cancer 19 (1) (2020) 130, https://doi.org/10.1186/s12943-020-01249-8.

[22] N. Hu, H. Ji, N6-methyladenosine (m6A)-mediated up-regulation of long noncoding RNA LINC01320 promotes the proliferation, migration, and invasion of gastric cancer via miR495-5p/RAB19 axis, Bioengineered 12 (1) (2021) 4081–4091, https://doi.org/10.1080/21655979.2021.1953210.

[23] J.X. Lin, N.Z. Lian, Y.X. Gao, Q.L. Zheng, Y.H. Yang, Y.B. Ma, Z.S. Xiu, Q.Z. Qiu, H.G. Wang, C.H. Zheng, P. Li, J.W. Xie, J. Lu, Q.Y. Chen, L.L. Cao, M. Lin, J. B. Wang, C.M. Huang, m6A methylation mediates LHPP acetylation as a tumour aerobic glycolysis suppressor to improve the prognosis of gastric cancer, Cell Death Dis 13 (5) (2022) 463, https://doi.org/10.1038/s41419-022-04859-w.

[24] S. Conic, D. Desplancq, A. Ferrand, V. Fischer, V. Heyer, B. Reina San Martin, J. Pontabry, M. Oulad-Abdelghani, N.K. Babu, G.D. Wright, N. Molina, E. Weiss, L. Tora, Imaging of native transcription factors and histone phosphorylation at high resolution in live cells, J Cell Biol 217 (4) (2018) 1537–1552, https://doi.org/10.1083/jcb.201709153.

[25] WS Jr Mohan, E. Scheer, O. Wendling, D. Metzger, L. Tora, TAF10 (TAF(II)30) is necessary for TFIID stability and early embryogenesis in mice, Mol Cell Biol 23 (12) (2003) 4307–4318, https://doi.org/10.1128/MCB.23.12.4307-4318.2003.

[26] J.Z. Ma, F. Yang, C.C. Zhou, F. Liu, J.H. Yuan, F. Wang, T.T. Wang, Q.G. Xu, W.P. Zhou, S.H. Sun, METTL14 suppresses the metastatic potential of hepatocellular carcinoma by modulating $N^6$ -methyladenosine-dependent primary MicroRNA processing, Hepatology 65 (2) (2017) 529–543, https://doi.org/10.1002/hep.28885.

[27] T. Sun, Z. Wu, X. Wang, Y. Wang, X. Hu, W. Qin, S. Lu, D. Xu, Y. Wu, Q. Chen, X. Ding, H. Guo, Y. Li, Y. Wang, B. Fu, W. Yao, M. Wei, H. Wu, Correction to: LNC942 promoting METTL14-mediated m 6 A methylation in breast cancer cell proliferation and progression, Oncogene 41 (11) (2022) 1677, https://doi.org/10.1038/s41388-022-02194-0.